

United States  
Naval Postgraduate School



THESIS

Response of a Water Column  
to  
Internal Waves of Known Frequencies

by

William John Lounsbery

Thesis Advisor:

J.A. Galt

September 1971

Thesis  
L827

*Approved for public release; distribution unlimited.*



# United States Naval Postgraduate School



## THESIS

Response of a Water Column  
to  
Internal Waves of Known Frequencies

by

William John Lounsbery

Thesis Advisor:

J.A. Galt

September 1971

*Approved for public release; distribution unlimited.*

T143 130



Response of a Water Column  
to  
Internal Waves of Known Frequencies

by

William John Lounsbery  
Lieutenant Commander, United States Navy  
B.S., Auburn University, 1963

Submitted in partial fulfillment of the  
requirements for the degree of

MASTER OF SCIENCE IN OCEANOGRAPHY

from the

NAVAL POSTGRADUATE SCHOOL  
September 1971



## ABSTRACT

A program is developed to ascertain the response of a frictionless water column to internal waves. Using density strata as input, the program selects ten frequencies at equal intervals within a spectrum of internal waves bounded above by the maximum Vaisala frequency and below by the inertial frequency. Ray paths within the column are plotted for these frequencies. The first ten normal modes for each frequency are computed. The first three modes are plotted.





## TABLE OF CONTENTS

I.	INTRODUCTION -----	7
II.	THEORY -----	11
	A. DEVELOPMENT OF THE INTERNAL WAVE EQUATION -----	11
	B. APPLICATION OF RAY THEORY -----	14
	C. NORMAL MODE APPLICATION -----	17
III.	DEVELOPMENT OF THE MODEL -----	20
	A. MAIN PROGRAM -----	20
	B. SUBROUTINE INTERP -----	20
	C. SUBROUTINE RAY -----	20
	D. SUBROUTINE RUNK -----	21
IV.	TESTING THE PROGRAM -----	23
	A. LINEAR INPUT -----	23
	B. THREE-LAYER INPUT -----	23
V.	APPLICATION OF THE PROGRAM TO OCEANOGRAPHIC DATA --	28
VI.	CONCLUSIONS -----	45
	APPENDIX - COMPUTER PROGRAM -----	46
	LIST OF REFERENCES -----	58
	INITIAL DISTRIBUTION LIST -----	59
	FORM DD 1473 -----	60



## LIST OF TABLES

Table I.	Comparison of Eigenvalues from Analytical and Numerical Solutions -----	24
Table II.	First Page of Computer Output for Deep Station -----	31
Table III.	Normal Modes Obtained for Deep Station -----	37
Table IV.	First Page of Computer Output for Shallow Station -----	38
Table V.	Normal Modes Obtained for Shallow Station ---	44



## LIST OF FIGURES

Figure 1.	Variation of Vaisala Frequency with Temperature Profile -----	9
Figure 2.	Illustration of Angle Between Horizontal and Phase Velocity -----	16
Figure 3.	Relation Between Phase and Group Velocities -	18
Figure 4.	Comparison of Eigenfunctions for First three Modes of Frequency 0.00684 -----	25
Figure 5.	Comparison of Vaisala Frequency Plots by Analytical and Numerical Methods -----	27
Figure 6.	Plot of Density Variation and Vaisala Frequency for the Deep Station -----	32
Figure 7.	Ray Paths for First Three Selected Frequencies of the Deep Station -----	33
Figure 8.	Ray Paths for Third through Sixth Frequencies of the Deep Station -----	34
Figure 9.	Modal Structure for First Three Modes of First Frequency at Deep Station -----	35
Figure 10.	Density and Vaisala Frequency at Shallow Station -----	39
Figure 11.	Ray Plots for First Two Selected Frequencies at Shallow Station -----	40
Figure 12.	Ray Plots for Third through Ninth Frequency at Shallow Station -----	41
Figure 13.	Modal Structures for First Selected Frequency at Shallow Station -----	42
Figure 14.	Modal Structure for Third Selected Frequency at Shallow Station -----	43



## ACKNOWLEDGEMENT

I sincerely thank Dr. Jerry Galt, friend as well as advisor, who not only presented the initial problem, packaged neatly, but who also spent many extra hours helping me unwrap it. To my wife, Janice, I give special thanks for aiding me in drafting the thesis and, particularly, for weathering the storm of neglect while I concentrated on the problem.





## I. INTRODUCTION

Internal waves exist in all oceans, most bays and lakes; they vary widely in amplitude, period, and depth (La Fond, 1962). Recently, advances have been made in interpreting the major features of the oceanic internal wave field (Wunsch and Dahlen, 1970).

Internal waves can be observed as density perturbations through a stable, stratified water column. Since temperature correlates with density in the majority of the upper ocean areas, internal waves often appear as oscillations about the region of the thermocline, exhibiting greatest amplitude and phase speed where the thermocline is the most intense. The oscillation initiated within the water column is described in terms of the Vaisala or stability frequency. This frequency may be derived as follows (Zalkan, 1966).

Consider the force acting on a water parcel raised vertically from its equilibrium position:

$$F = g[\rho - (\rho + \frac{\partial \rho}{\partial Z} \Delta Z)]dV - \rho \frac{g^2}{c^2} \Delta Z dV \quad (1)$$

where:  $g$  = gravitational acceleration,

$\rho$  = density,

$\Delta Z$  = vertical displacement,

$dV$  = minute volume of the parcel, and

$c$  = sound velocity. The first term on the right hand side is the restoring force due to buoyancy. The second term is the contributing force of compressibility. The equation



for the induced vertical motion is:

$$\rho dV \frac{dz^2}{dz^2} = -g \frac{\partial \rho}{\partial z} z dV - \rho \frac{g^2}{c^2} z dV \quad (2)$$

The harmonic solution to equation (2) is the Vaisala frequency defined as

$$N(Z) = \sqrt{\frac{-g}{\rho} \frac{\partial \rho}{\partial z} - \frac{g^2}{c^2}} \quad (3)$$

For oceanographic applications the water is effectively incompressible and the second term under the radical is negligible. Thus,

$$N(Z) = \sqrt{\frac{-g}{\rho} \frac{\partial \rho}{\partial z}} \quad (4)$$

The Vaisala frequency is greatest in magnitude where the thermocline is most intense (see Figure 1).

The vertical motion initiated by the internal wave passing through the water column is governed by the differential equation (Fjeldstad, 1933):

$$\frac{\partial}{\partial z} \left( \rho \frac{dW}{dz} \right) + \frac{k^2}{\sigma^2 - f^2} (N^2 - \sigma^2) W = 0 \quad (5)$$

where:  $W$  = vertical water velocity,

$k$  = internal wave number,

$\sigma$  = internal wave frequency, and

$f$  = inertial frequency. Equation (5) is a hyperbolic wave equation whose characteristics describe the direction of propagation of internal wave energy. With the appropriate boundary conditions that no vertical flow exists at the surface or at the bottom, the internal wave equation satisfies the criteria for a Sturmian system. The imposed boundary



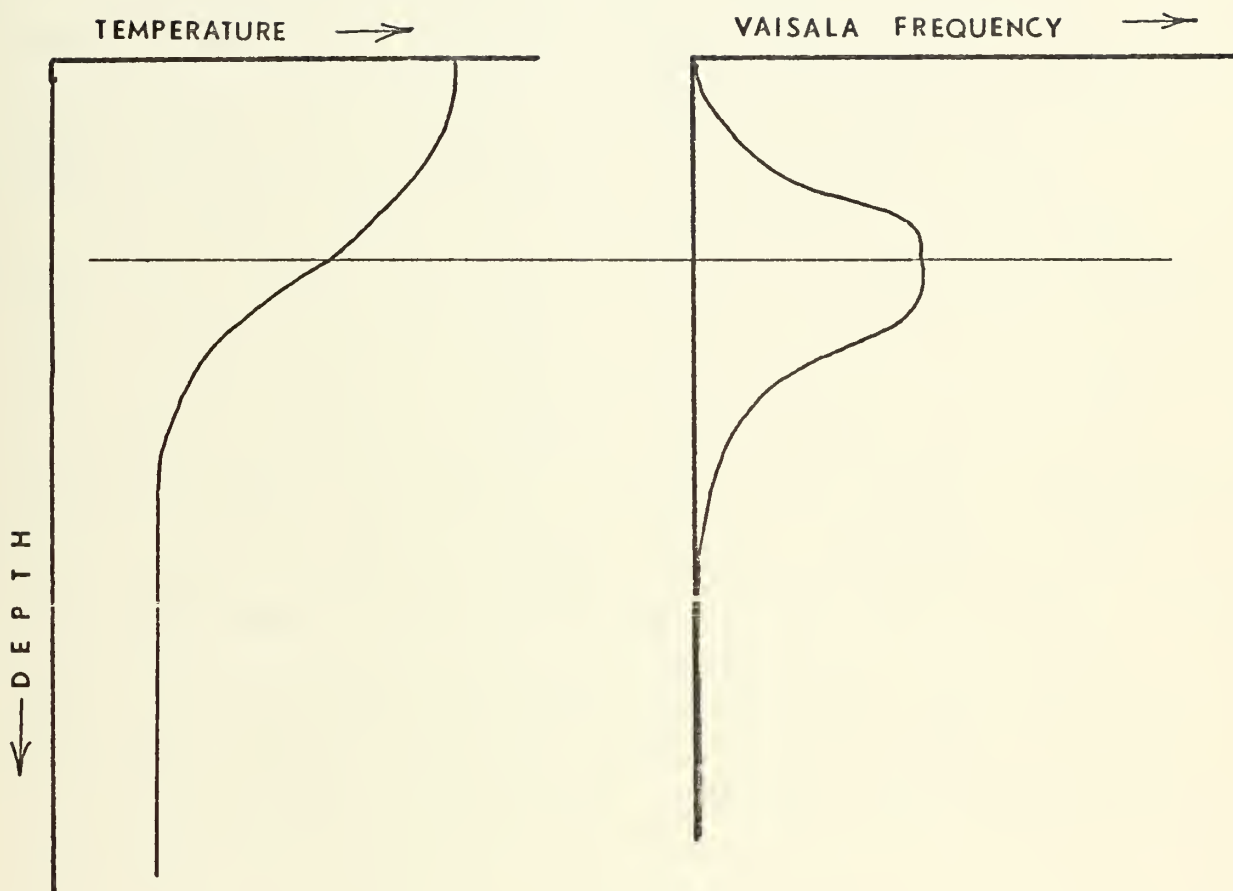


FIGURE 1. Variation of Vaisala Frequency with Temperature Profile



conditions are satisfied by the simultaneous propagation of two waves having the same horizontal wave number, one with its vertical component of phase velocity up, the other with its vertical component down. The stipulation that these waves cancel at the boundaries leads to the structure of normal modes. These modes constitute a discrete set of wave numbers that are the eigenvalues of the Sturmian system.

This thesis, using as a basis Fjeldstad's classic paper (Fjeldstad, 1933), developed a numerical program that assessed the response by a frictionless, incompressible water column to internal waves in a frequency band bounded above by the maximum Vaisala frequency and below by the inertial frequency. Station density strata was used as input. Frequencies were selected within the band and their ray paths were drawn. Also, the governing differential equation was numerically integrated and the resulting endpoints were refined to determine the first ten normal modes. The first three modes were plotted.

The program was first tested using density strata with known output. The program then treated data taken from ocean stations off the coast of Monterey, California in mid-August, 1970.





## II. THEORY

### A. DEVELOPMENT OF THE INTERNAL WAVE EQUATION

For a frictionless, incompressible water column the governing equations (following Feldstad, 1933) are:

Momentum

$$\frac{\partial U}{\partial t} - fV + \frac{1}{\rho} \frac{\partial P}{\partial X} = 0 \quad (6)$$

$$\frac{\partial V}{\partial t} + fU + \frac{1}{\rho} \frac{\partial P}{\partial Y} = 0 \quad (7)$$

$$\frac{\partial W}{\partial t} + g + \frac{1}{\rho} \frac{\partial P}{\partial Z} = 0 \quad (8)$$

Continuity

$$\frac{\partial U}{\partial X} + \frac{\partial V}{\partial Y} + \frac{\partial W}{\partial Z} = 0 \quad (9)$$

Density invariant

$$\frac{\partial \rho}{\partial t} + U \frac{\partial \rho}{\partial X} + V \frac{\partial \rho}{\partial Y} + W \frac{\partial \rho}{\partial Z} = 0 \quad (10)$$

The X-axis is directed in the direction of wave travel, the Y-axis is in the horizontal transverse plane of travel, and the Z-axis is vertical, positive upward. U, V, and W are the velocity components of the water in the X, Y, and Z axes, respectively. f is the coriolis parameter. P is the pressure. The depth is assumed to be uniform. Z=0 is the bottom; Z=h is the undisturbed upper surface. For a steady state condition,

$$\frac{dU}{dt} = \frac{dV}{dt} = \frac{dW}{dt} = 0. \quad (11)$$

Thus,

$$dP = -\rho g dZ. \quad (12)$$



P can be represented as

$$P = P_0 + g \int_z^h \rho dz, \quad (13)$$

where  $P_0$  is the undisturbed pressure at the surface. Let

$$\rho = \rho_0(Z) + \rho_1(X, Y, Z, t), \quad (14)$$

where  $\rho_0$  is the undisturbed density and  $\rho_1$  the perturbation.

Therefore, pressure for the perturbation is:

$$P = P_0 + g \int_z^h \rho_0 dZ + P_1 \quad (15)$$

where

$$P_1 = g \int_h^z \rho_1 dZ \quad (16)$$

Invoking a general assumption that velocities and perturbations of density and pressure are small enough that their products and squares may be neglected, equation (10) may be written:

$$\rho_0 \frac{1}{\sigma} \frac{\partial P_1}{\partial t} + \rho_0 \frac{1}{\sigma} \frac{\partial \rho_0}{\partial Z} W = 0 \quad (17)$$

If, for the internal wave form, harmonic oscillations such as the following are considered:

$$u, \rho_1, P_1 \approx \cos(\sigma t - kx) \exp(ay)$$

$$v, w \approx \sin(\sigma t - kx) \exp(ay)$$

where the constant  $a$  controls the transverse envelope and allows for the possibility of edge waves. The sign of  $a$  is such that the wave amplitude decays away from the boundary.

The governing equations now become:

$$\sigma U - fV + k \frac{P_1}{\rho_0} = 0 \quad (18)$$

$$\sigma V + fU + a \frac{P_1}{\rho_0} = 0 \quad (19)$$



$$\sigma^W + g + \frac{1}{\rho_0} \frac{\partial P_1}{\partial Z} = 0 \quad (20)$$

$$kU + aV + \frac{dW}{dZ} = 0 \quad (21)$$

Solving equations (18) and (19) for U and V:

$$U = \frac{k + fa}{\sigma^2 - f^2} \frac{P_1}{\rho_0} \quad (22)$$

$$V = \frac{fk + a}{\sigma^2 - f^2} \frac{P_1}{\rho_0}. \quad (23)$$

Solving for the vertical pressure gradient:

$$\frac{dP_1}{dZ} = \frac{N^2 - \sigma^2}{\sigma} \rho_0 W \quad (24)$$

where  $N^2 = -\frac{g}{\rho_0} \frac{d\rho_0}{dZ}$  as previously defined. When one inserts (22) and (23) in (9):

$$\frac{P_1}{\rho_0} = -\frac{(\sigma^2 + f^2)}{\sigma(k^2 - a^2)} \frac{dW}{dZ}. \quad (25)$$

When  $P_1$  is eliminated from (24) and (25) and the transverse boundaries are disregarded (i.e., set  $a=0$ ),

$$\frac{d^2 W}{dZ^2} + \left(\frac{1}{\rho_0} \frac{d\rho_0}{dZ}\right) \frac{dW}{dZ} + \left[\frac{k^2}{\sigma^2 - f^2}\right] [N^2 - \sigma^2] W = 0 \quad (26)$$

Equation (26) is the internal wave equation describing the response by a water column to a plane internal wave of known frequency,  $\sigma$ . The order of magnitude of the second term is small compared to the first and third. However, the numerical program can include the second term without any difficulty. It will be so retained.



## B. APPLICATION OF RAY THEORY

An analytical solution to equation (26) may be made by the transformation:

$$W = (Z) \exp \left( \frac{1}{\rho_0} \frac{\partial \rho_0}{\partial Z} \frac{Z}{2} \right). \quad (27)$$

When the effect of the second term in eq. (26) is small, the analytical solution to the internal wave equation can, with a high degree of accuracy, be represented by  $\Psi$ , the oscillatory portion. The oscillatory solution is:

$$\Psi_{ZZ} + \left( \frac{k^2}{\sigma^2 - f^2} \right) (N^2 - \sigma^2) W = 0 \quad (28)$$

Solutions to equation (28) are of the form:

$$\Psi = A \exp i \left( k_1 X \pm k_1 \frac{N^2 - 2}{\sigma^2 - f^2} Y \pm \sigma t \right) \quad (29)$$

where  $k_1$  = horizontal wave number.

Define  $\Theta$  as the angle between the horizontal and the phase velocity. Then,

$$\cos \Theta = \frac{k_1}{(k_1^2 + k_1^2 \left[ \frac{N^2 - \sigma^2}{\sigma^2 - f^2} \right])^{1/2}} = \left[ \frac{\sigma^2 - f^2}{N^2 - f^2} \right]^{1/2} \quad (30)$$

Since

$$(\sigma^2 - f^2)^{1/2} = (N^2 - \sigma^2)^{1/2} \frac{k_1}{(k_1^2 + k_2^2)^{1/2}} \quad (31)$$

$$\sigma = \left[ \frac{k_1^2 N^2 + k_2^2 f^2}{k_1^2 + k_2^2} \right]^{1/2} \quad (31a)$$

where

$$k_2 = k_1 \left( \frac{N^2 - 2}{\sigma^2 - f^2} \right)^{1/2} \quad (32)$$

$$|k| = (k_1^2 + k_2^2)^{1/2} \quad (33)$$





Figure 2 illustrates the angle between the horizontal and the phase velocity. The phase velocity, broken into X and Z components, is:

$$C_X = \frac{k_1}{k_1^2 + k_2^2} = \frac{k_1}{(k_1^2 + k_2^2)^{3/2}} [k_1^2 N^2 + k_2^2 f^2]^{1/2} \quad (34)$$

and

$$C_Z = \frac{k_2}{(k_1^2 + k_2^2)^{3/2}} [k_1^2 N^2 + k_2^2 f^2]^{1/2} \quad (35)$$

For the group velocity,

$$\vec{C}_g = \nabla_k \sigma \quad (36)$$

where

$$\nabla_k = \left( \frac{\partial}{\partial k_1} \vec{i} + \frac{\partial}{\partial k_2} \vec{j} \right) \quad (37)$$

$$\vec{C}_g = \nabla_k \left[ \left( \frac{k_1^2 N^2 + k_2^2 f^2}{k_1^2 + k_2^2} \right)^{1/2} \right] \quad (38)$$

The X-component of group velocity is:

$$\begin{aligned} (C_g)_X &= \frac{\partial}{\partial k_1} \left[ \left( \frac{k_1^2 N^2 + k_2^2 f^2}{k_1^2 + k_2^2} \right)^{1/2} \right] \\ &= \frac{k_1 k_2^2}{|k|^3} \left[ \frac{(N^2 - f^2)}{(k_1^2 N^2 + k_2^2 f^2)^{1/2}} \right] \end{aligned} \quad (39)$$

The Z-component of group velocity is:

$$\begin{aligned} (C_g)_Z &= \frac{\partial}{\partial k_2} \left[ \left( \frac{k_1^2 N^2 + k_2^2 f^2}{k_1^2 + k_2^2} \right)^{1/2} \right] \\ &= -\frac{k_1^2 k_2}{|k|^3} \left[ \frac{(N^2 - f^2)}{(k_1^2 N^2 + k_2^2 f^2)^{1/2}} \right] \end{aligned} \quad (40)$$

Define  $\Theta_g$  as the angle made with the horizontal by the group velocity vector. Then,



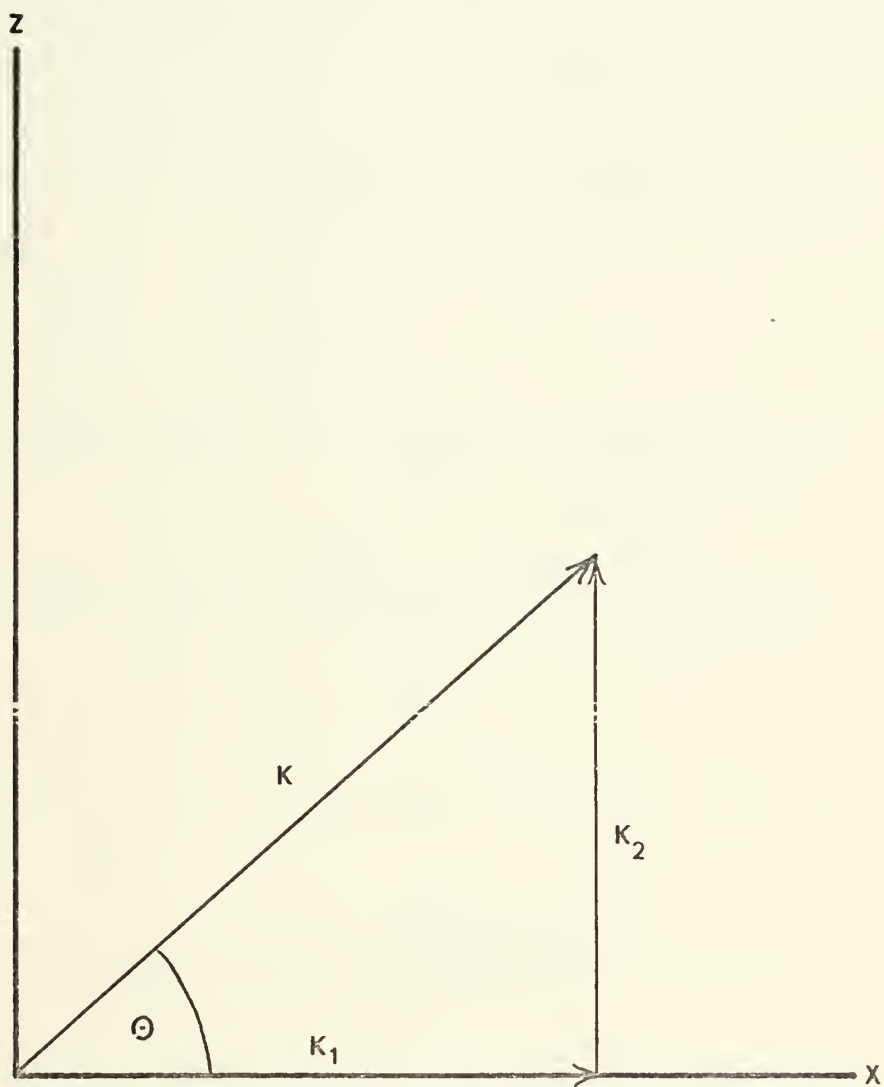


FIGURE 2. Illustration of Angle between Horizontal and Phase Velocity



$$\tan \Theta_g = \frac{(C_g)_Z}{(C_g)_X} = \frac{-K_1}{K_2} = \left[ \frac{N^2 - f^2}{\sigma^2 - f^2} \right]^{1/2} \quad (41)$$

The ray trace part of the program drew the ray paths as depicted in equation (41) for ten frequencies selected within the inertio-gravity band.

Determining the dot product of the phase and group velocities:

$$\begin{aligned} \vec{C} \cdot \vec{C}_g &= \\ & \left( \frac{k_1(k_1^2 N^2 + k_2^2 f^2)^{1/2}}{|k|^3} \right) \left( \frac{k_1 k_1^2}{|k|^3} \frac{(N^2 - f^2)}{(k_1^2 N^2 + k_2^2 f^2)^{1/2}} \right) \\ & - \left( \frac{k_2(k_1^2 N^2 + k_2^2 f^2)^{1/2}}{|k|^3} \right) \left( \frac{k_1^2 k_2 (N^2 - f^2)}{|k|^3 (k_1^2 N^2 + k_2^2 f^2)^{1/2}} \right) \\ & = 0 \end{aligned} \quad (42)$$

Thus the phase velocity is perpendicular to the group velocity. Also,

$$C_Z + (C_g)_Z = \frac{k_2(k_2^2 - k_1^2)f^2}{(k_1^2 N^2 + k_2^2 f^2)^{1/2} (k_1^2 + k_2^2)^{3/2}} \quad (43)$$

The phase velocity and group velocity then have a relationship as seen in Figure 3.

### C. NORMAL MODE APPLICATION

With the use of suitable boundary conditions, equation (26) may be solved to obtain modal structures. The applicable conditions are:

$$W = 0 \quad \text{at} \quad Z = 0 \quad (44)$$



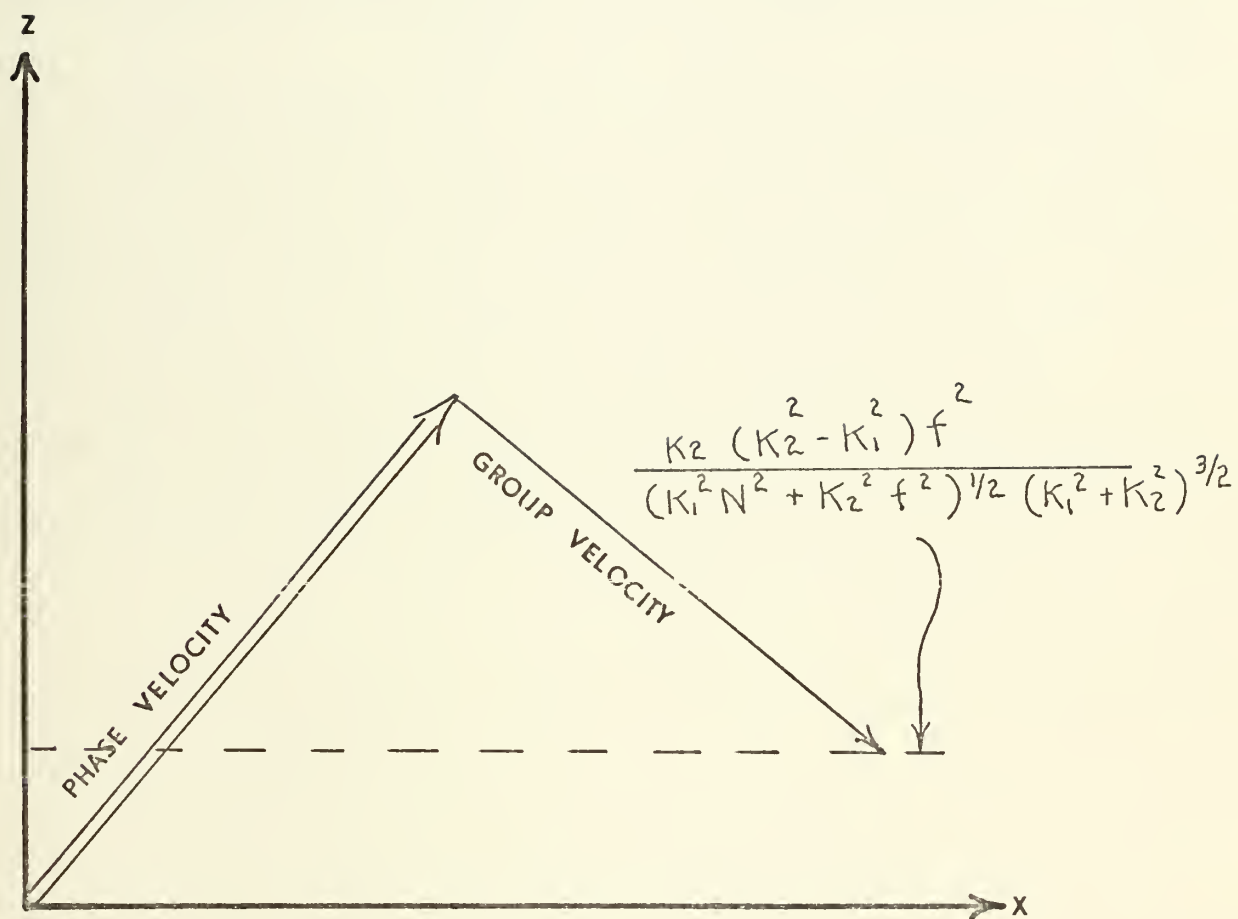


Figure 3. Relation between Phase and Group Velocities





and

$$\frac{dW}{dZ} - \frac{k^2}{\sigma^2 - f^2} gW = 0 \quad \text{at} \quad Z = h \quad (44a)$$

To a high degree of approximation the vertical velocity shear is negligible at the surface and the second condition becomes:

$$W = 0 \quad \text{at} \quad Z = h \quad (45)$$

Equations (26), (44), and (45) compose a Sturmian system.  $W$ , the vertical velocity, is the eigenfunction. For a given frequency, discrete wave numbers or eigenvalues are determined. The program utilized a fourth-order Runge-Kutta numerical method to obtain an end value after integration of the internal wave equation over the water column. The endpoint was refined using a Newton-Raphson iteration procedure.



### III. DEVELOPMENT OF THE MODEL

#### A. MAIN PROGRAM

The main program prints the station density stratification. The program then calls upon the three sub-programs to interpolate density between station depths, to plot ray paths for selected internal wave frequencies, and to print out and plot modal structures for these frequencies.

#### B. SUBROUTINE INTERP

Subroutine INTERP interpolates the density stratification for 400 incremental depths through the water column. The interpolation is accomplished by the use of a third-degree polynomial that matches points and slopes at each depth where data was obtained from a Nansen bottle. To guarantee density stability, the smaller of the slope above or below each point is chosen as the slope at that point. From the interpolation polynomial, INTERP computes the Vaisala frequency for each density value.

#### C. SUBROUTINE RAY

Subroutine RAY plots the interpolated density and the Vaisala frequency as a function of depth. RAY then determines the inertio-gravity frequencies at rates of  $1/100$ ,  $1/10$ ,  $2/10$ ,  $3/10$ ,  $4/10$ ,  $5/10$ ,  $6/10$ ,  $7/10$ ,  $8/10$ , and  $9/10$  of the frequency band. The program then plots the characteristic paths over the depth of the column for each of these frequencies.



Additionally, subroutine RAY determines the percentage of the water column depth where the selected frequency exceeds the Vaisala frequency. This percentage represents that portion of the column where the Sturmian solution to the internal wave equation is exponential. A greater percentage implies increasing difficulty in applying boundary conditions during the numerical integration. The percentage figure for each frequency is listed beneath the ray path plot.

#### D. SUBROUTINE RUNK

Subroutine RUNK utilizes a fourth-order Runge-Kutta numerical method to integrate the internal wave equation over the water column. The endpoint of the integration is refined by a Newton-Raphson iteration method until the endpoint is 1/200 of the maximum value of the eigenfunction,  $W$ , determined during the integration scheme. For each selected frequency, the first approximation for the initial eigenvalue is

$$K_1 = \frac{\sigma}{\sqrt{gh}} \quad (45)$$

The approximation is refined until the wave number corresponding to the first mode is determined. The approximation for the second mode is twice the value of  $K_1$ . The initial estimate of the remaining eight eigenvalues is the previous eigenvalue plus the difference between the previous two eigenvalues.

After the first three eigenvalues are determined, the program plots their modal structure. The remaining seven wave numbers are then listed.



As the selected frequencies within the inertio-gravity band increase in magnitude, the boundary constraints, though analytically well-defined, weaken exponentially. The higher frequencies are greater than the incremental Vaisala frequency for a greater percentage of column depth and it becomes increasingly difficult for the numerical program to find eigenvalues. RUNK terminates its search for the next eigenvalues by (1) stopping after 20 refinements by the Newton-Raphson iteration process, (2) restricting the magnitude of the eigenfunction to  $10^{20}$  cm/sec, and (3) stopping if the solution converges to a mode other than the one searched for.

Also, as the frequency within the band increases,  $W$  becomes more sensitive to changes in  $k$  when seeking higher modes. For situations where a minute change in  $k$  causes abrupt responses in end values of  $W$ , the eigenvalue may be only refined to a certain degree. These eigenvalues are indicated as approximations.





#### IV. TESTING THE PROGRAM

##### A. LINEAR INPUT

To check numerical formulation, coding, and accuracy, two test cases were used whose analytic solutions were possible. The first test was a linear variation of depth from 1.023 grams/cc at the surface to 1.033 grams/cc at the bottom depth of 1000 meters. The Vaisala frequency for this input was constant and equal to:

$$\begin{aligned} N &= \sqrt{-\frac{g}{\rho} \frac{\partial \rho}{\partial z}} \\ &= \sqrt{\frac{9.8 \text{ M/sec}^2}{1.025 \cdot 614/\text{cc}}} \times 10^{-5} = 9.77 \times 10^{-3} \text{ sec}^{-1}. \end{aligned} \quad (46)$$

The plot by the program of the density matches that of the linear variation. The Vaisala frequency determined numerically matches that determined analytically. Table I compares the analytical and numerical results of the linear variation of density for frequency 0.00684 cycles/min. Figure 4 compares the first three modal structures. Analytically, the normal modes are

$$K_m = \left( \frac{\sigma^2 - f^2}{N^2 - f^2} \right)^{1/2} \left( \frac{m\pi}{h} \right). \quad (47)$$

The eigenfunction is:

$$\exp \left( \frac{N^2}{g} \frac{z}{2} \right) \sin \left( \frac{m\pi}{h} z \right) \quad (48)$$

##### B. THREE-LAYER INPUT

The second input was a density strata that was constant at 1.023 grams/cc from the surface to 300 meters, varied



Table I. A comparison of the first ten normal modes determined for frequency 0.00684 cycles/min:

	<u>Analytical</u>	<u>Numerical</u>	<u>% Error</u>
$k_1$	$3.613 \times 10^{-5}$	$3.629 \times 10^{-5}$	0.45
$k_2$	$7.225 \times 10^{-5}$	$7.259 \times 10^{-5}$	0.47
$k_3$	$1.083 \times 10^{-4}$	$1.088 \times 10^{-4}$	0.27
$k_4$	$1.445 \times 10^{-4}$	$1.451 \times 10^{-4}$	0.42
$k_5$	$1.806 \times 10^{-4}$	$1.814 \times 10^{-4}$	0.44
$k_6$	$2.167 \times 10^{-4}$	$2.177 \times 10^{-4}$	0.46
$k_7$	$2.529 \times 10^{-4}$	$2.540 \times 10^{-4}$	0.43
$k_8$	$2.890 \times 10^{-4}$	$2.903 \times 10^{-4}$	0.45
$k_9$	$3.251 \times 10^{-4}$	$3.266 \times 10^{-4}$	0.46
$k_{10}$	$3.613 \times 10^{-4}$	$3.629 \times 10^{-4}$	0.44



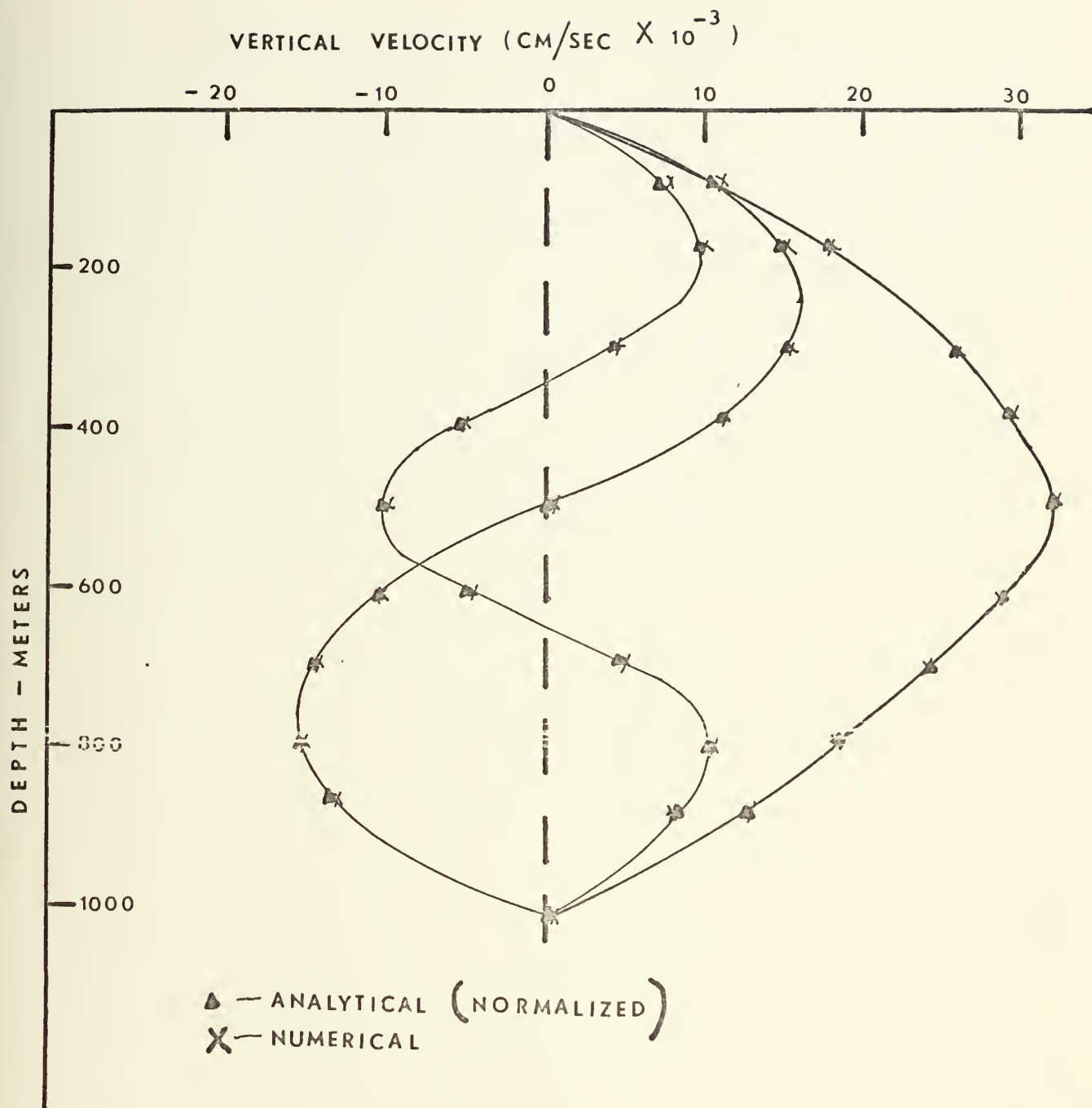


FIGURE 4. Comparison of Eigenfunctions for First 3 Modes of Frequency 0.00684



linearly from 300 meters to a value of 1.027 grams/cc at 700 meters, and then remained invariant from 700 meters to the bottom at a depth of 1000 meters. The corresponding value of the Vaisala frequency was then zero in the upper and lower isopycnal layers and equal to  $9.8 \times 10^{-3}$  in the middle region.

The density plot by the program matched the analytic solution to the third decimal place. Figure 5 illustrates the comparison between the analytic solution and the computer solution for the Vaisala frequency, and illustrates how the interpolation scheme handles discontinuities in the density slope.





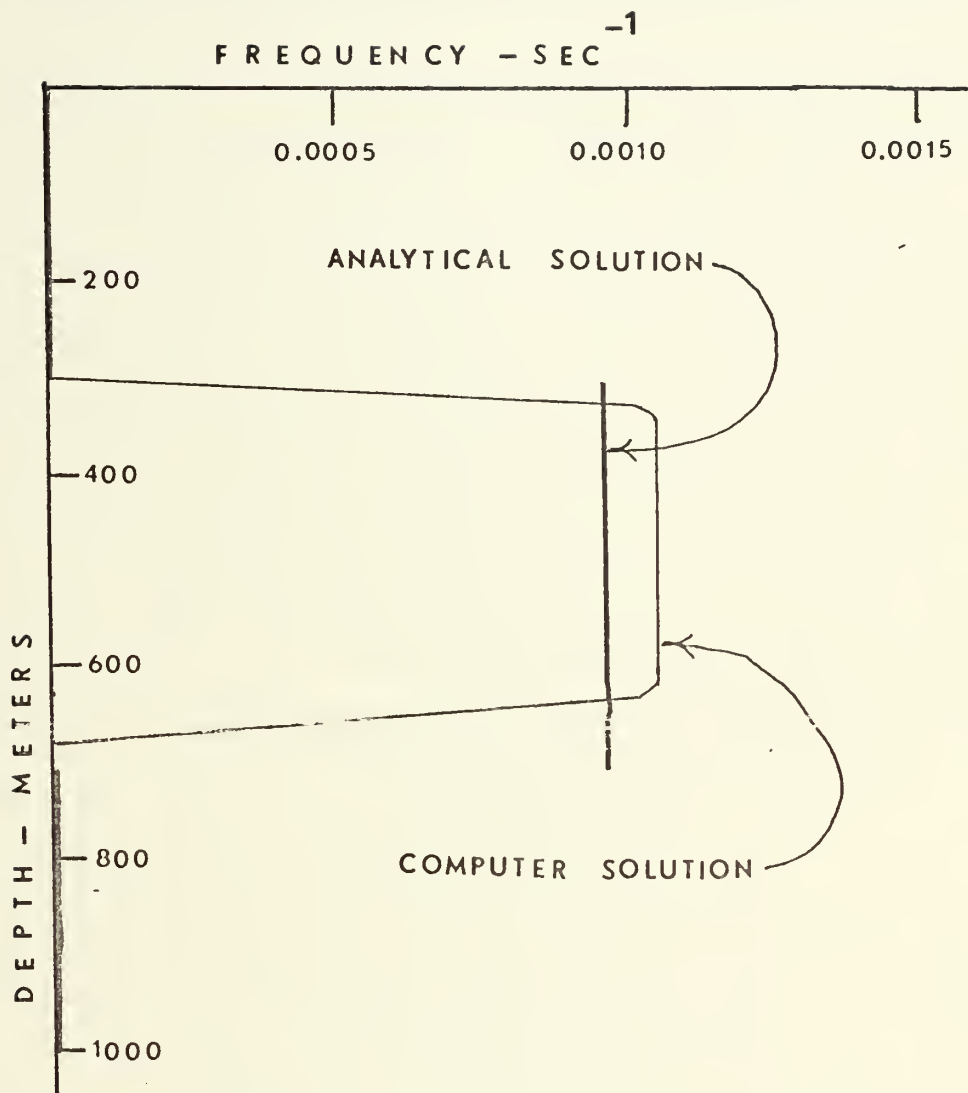


FIGURE 5. Comparison of Vaisala Frequency Plots by Analytical and Numerical Methods



## V. APPLICATION OF THE PROGRAM TO OCEANOGRAPHIC DATA

The program utilizes density strata from Nansen casts. It can process several stations. IDATA, the number of stations to be studied, is the first card to be typed. It follows the alphanumerics that are read in and serves in the plotting portions of the program. IDATA is read in as an integer, right-oriented to column ten of the IBM card. The second card to be typed up consists of three figures. The first is M, the number of bottles at the station, read in as an integer, right-oriented to column 10. The second is ZMAX, the depth at which the last bottle was taken, read in the format F10.1, right-oriented to column 20. The third figure is RLAT, the latitude of the station, that is read in using format F10.1 right-oriented to column 30.

The next cards to be typed are those representing the density strata. These are read in as four pairs of numbers for each card. Each number has a field width of ten and is right-oriented. The first number in each pair represents station depth and has a format of F10.1. The second of the pair has a format F10.5 and represents the station density. These four pairs of numbers, representing 80 columns per card, are entered until all the station data has been read in.

The above represent all the cards needed to be typed for each station. From experience gained using the IBM 360 computer to process ocean stations taken in mid-August, 1970,



off Monterey, California, it appears that two minutes are required to process shallower stations (around 200 meters) and four minutes to process deeper stations (around 2000 meters).

The actual printed output for each station appears as follows. On the first page of printed output appears:

(1) the number of station depths, (2) the lowest bottle depth, (3) a printout of the station depths and densities in columnar form, (4) the inertial frequency computed for the station, (5) the maximum Vaisala frequency computed for the station, and (6) the ten frequencies within the inertio-gravity band selected for consideration.

The second page of printed output plots the Vaisala frequency and density versus depth.

The next ten pages plot the ray path for each frequency versus depth. At the bottom of each ray plot, the amount of time that the frequency is greater than the Vaisala frequency is indicated.

The remaining twenty pages of output display information on normal modes. Corresponding to each of the ten selected frequencies are two pages. The first page lists the first three normal modes and plots these modes versus depth. The second page lists the remaining seven modes.

Two stations, one shallow and one deep, were chosen to illustrate the output from the program. The results for both stations are summarized by the following tables and figures.



Table II lists the information for the deep oceanographic station displayed on the first page of computer output. This station is representative of an oceanic internal wave regime. Figure 6 shows the plot of the density variation and the Vaisala frequency for the deep station. The Vaisala plot follows the pattern of the density profile.

Figure 7 depicts the ray paths for the first three selected frequencies. The first frequency selected, 0.01371 cycles/min, never exceeds the incremental Vaisala frequency. Thus, theoretically, its solution is always oscillatory and it travels horizontally nearly 30 km. The second frequency selected, 0.12969 cycles/min, exceeds the Vaisala frequency in the region of the water column below a depth of 970 meters. Thus it exponentially 'decays' in this region and its ray path over this portion of the water column is vertical. Figures 7 and 8 illustrate that, with increasing frequency, the horizontal distance covered by the ray path decreases and a greater portion is in the exponential region. The ray paths for the last four selected frequencies were not shown since their ray is nearly vertical from top to bottom.

Figure 9 plots the first three modes for frequency 0.01371 cycles/min. This was the only frequency for which the first three normal modes could be positively identified. Besides gaining a better understanding of the actual appearance of the modal structures, Figure 9 suggests optimum placement of a thermocline follower for mode detection. For example, the follower would best detect mode three at a depth of about





TABLE II. Data display for deep station.

<u>Incremental depth</u>	<u>Incremental density</u>
0.0	1.02498
10.0	1.02505
20.0	1.02522
30.0	1.02565
50.0	1.02588
75.0	1.02611
100.0	1.02624
150.0	1.02646
200.0	1.02656
300.0	1.02679
400.0	1.02681
500.0	1.02702
600.0	1.02711
800.0	1.02730
1000.0	1.02743
1200.0	1.02750
1500.0	1.02759
2000.0	1.02770
2500.0	1.02774
3000.0	1.02776

<u>Frequency number</u>	<u>Cycles/min</u>
inertial	0.00082
1	0.01371
2	0.12969
3	0.25855
4	0.38741
5	0.51628
6	0.64514
7	0.77401
8	0.90287
9	1.03173
10	1.16059
maximum Vaisala	1.28946



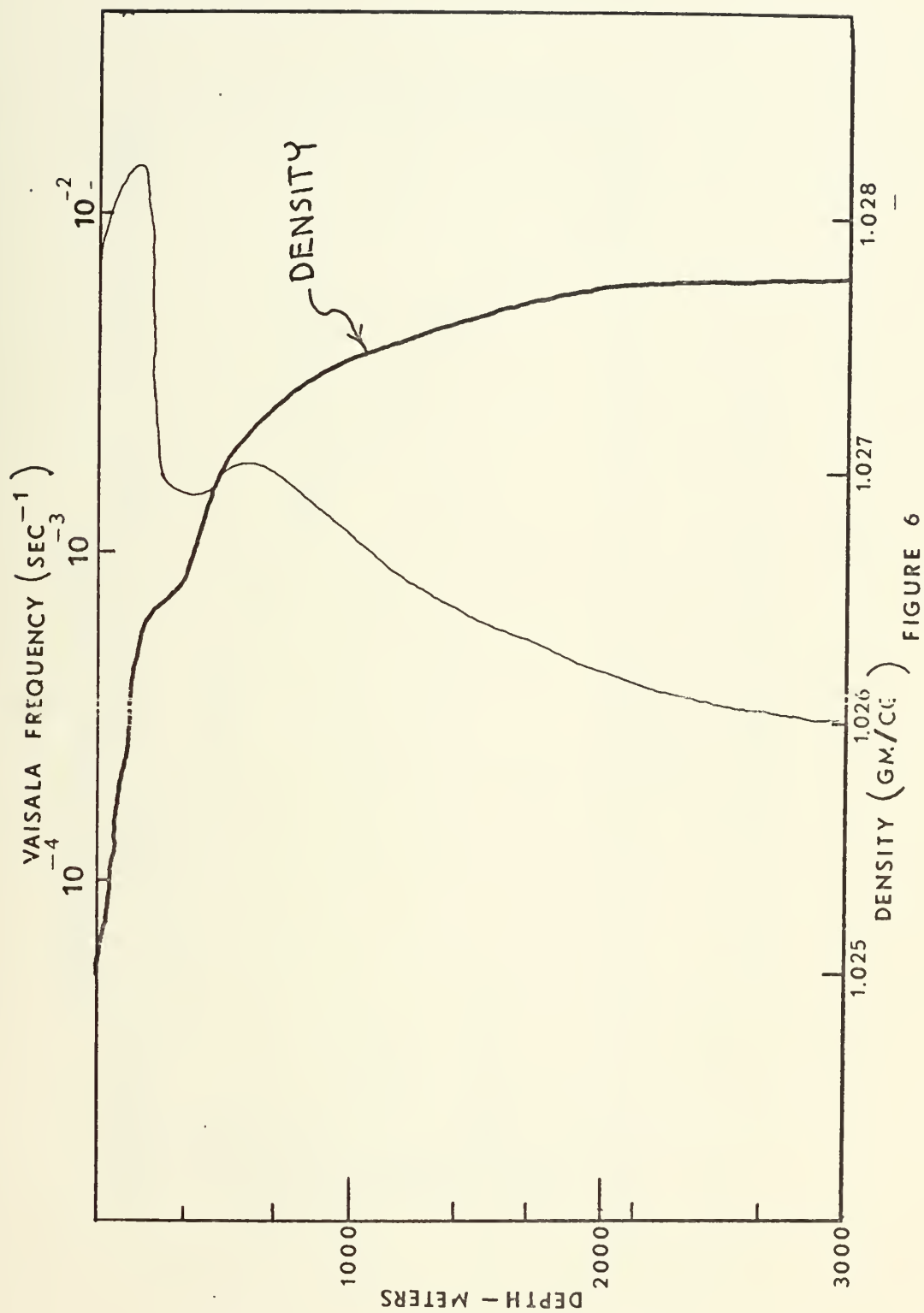


FIGURE 6. Density variation and Vaisala frequency for deep station



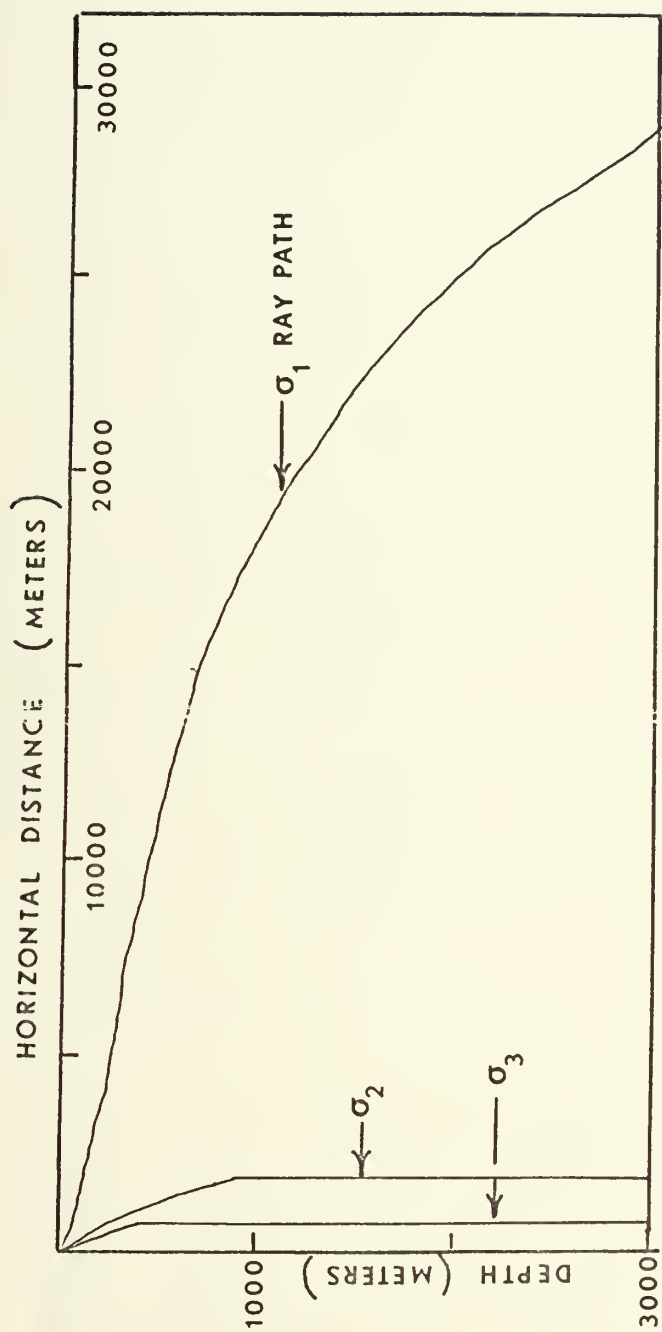


FIGURE 7

FIGURE 7. Ray paths for deep station



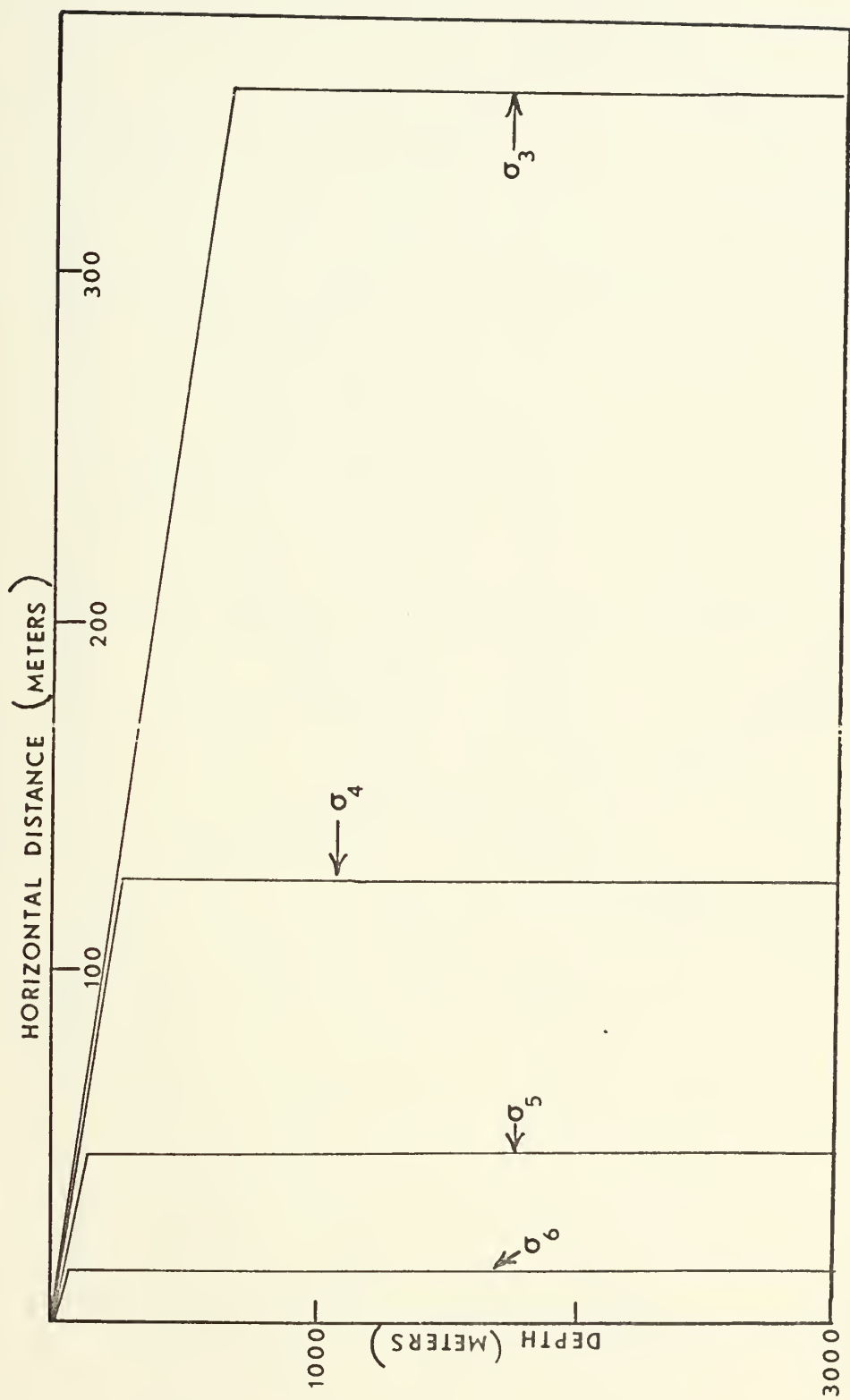


FIGURE 8. Ray paths for third through sixth frequency at deep station.





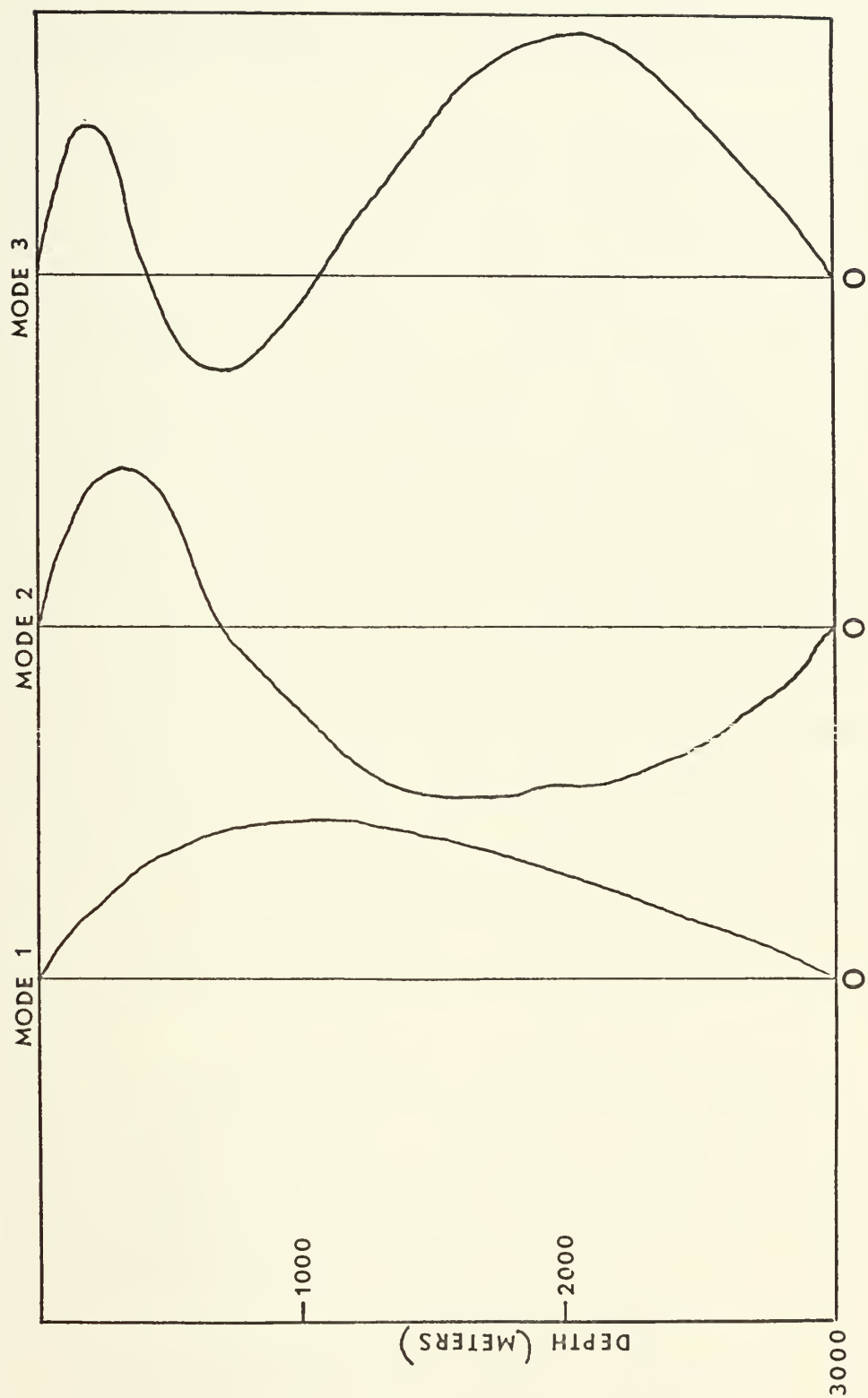


FIGURE 9. Modal structures for first three modes of first frequency



2000 meters. Table III lists the various modes determined for the selected frequencies for the deep oceanographic station.

Table IV displays the first page of printed output for the shallow station representative of the regime in a large bay. Figure 10 illustrates the density variation and the Vaisala frequency as a function of depth. As in the deep station, the first selected frequency of the shallow station has an oscillatory solution throughout most of the water column. Its ray path travels horizontally nearly 2500 meters. Its exponential region may be seen as a vertical path at a distance of 1955 meters. Figure 11 shows the effect of an increase in frequency without a considerable increase in the effect of exponential decay. The second frequency selected, 0.15818 cycles/min., has an exponential solution over the water column in nearly the same region as the first. However, frequency 2 only travels a horizontal distance of 230 meters. Figure 12 depicts the decrease in ray path as the frequency increases.

Figure 13 depicts the first three normal modes for frequency 0.01656 cycles/min. Figure 14 illustrates the first three normal modes for frequency 0.31554 cycles/min. Figure 14 illustrates well the manner in which the modal structure deteriorates with increased frequency. Table V lists the modes determined for selected frequencies at the shallow station.



Table III. Normal modes for selected frequencies at the deep station.

<u>0.01371 cycles/min.</u>	<u>0.12969 cycles/min.</u>
1. 0.00011736	1. 0.0018469
2. 0.00023344	2. 0.0034051
3. 0.00032185	
4. 0.00043948	
5. 0.00055503	
6. 0.00063828	
7. 0.00079211	
8. 0.00085791	
9. 0.00096286	
10. 0.00011641	



Table IV. Data display for shallow station.

<u>Incremental depth</u>	<u>Incremental density</u>
0.0	1.02535
5.0	1.02537
10.0	1.02543
15.0	1.02551
20.0	1.02570
25.0	1.02580
30.0	1.02606
40.0	1.02610
50.0	1.02614
60.0	1.02614
75.0	1.02616
100.0	1.02619

<u>Frequency number</u>	<u>Cycles/min</u>
inertial	0.00083
1	0.01656
2	0.15818
3	0.31554
4	0.47289
5	0.63024
6	0.78760
7	0.94495
8	1.10231
9	1.25966
10	1.41702
maximum Vaisala	1.57437





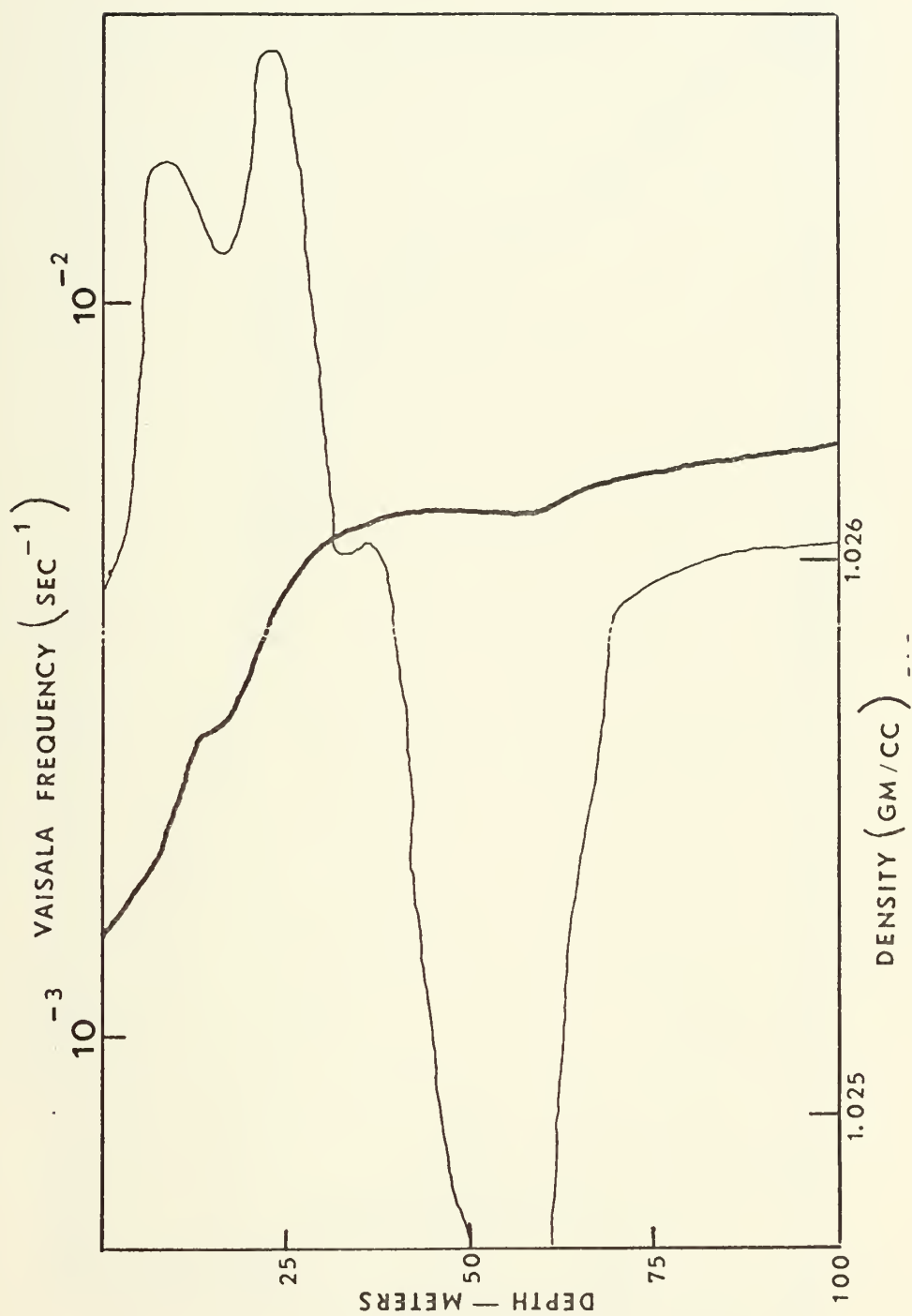


FIGURE 10. Density profile and Vaisala frequency at the shallow station



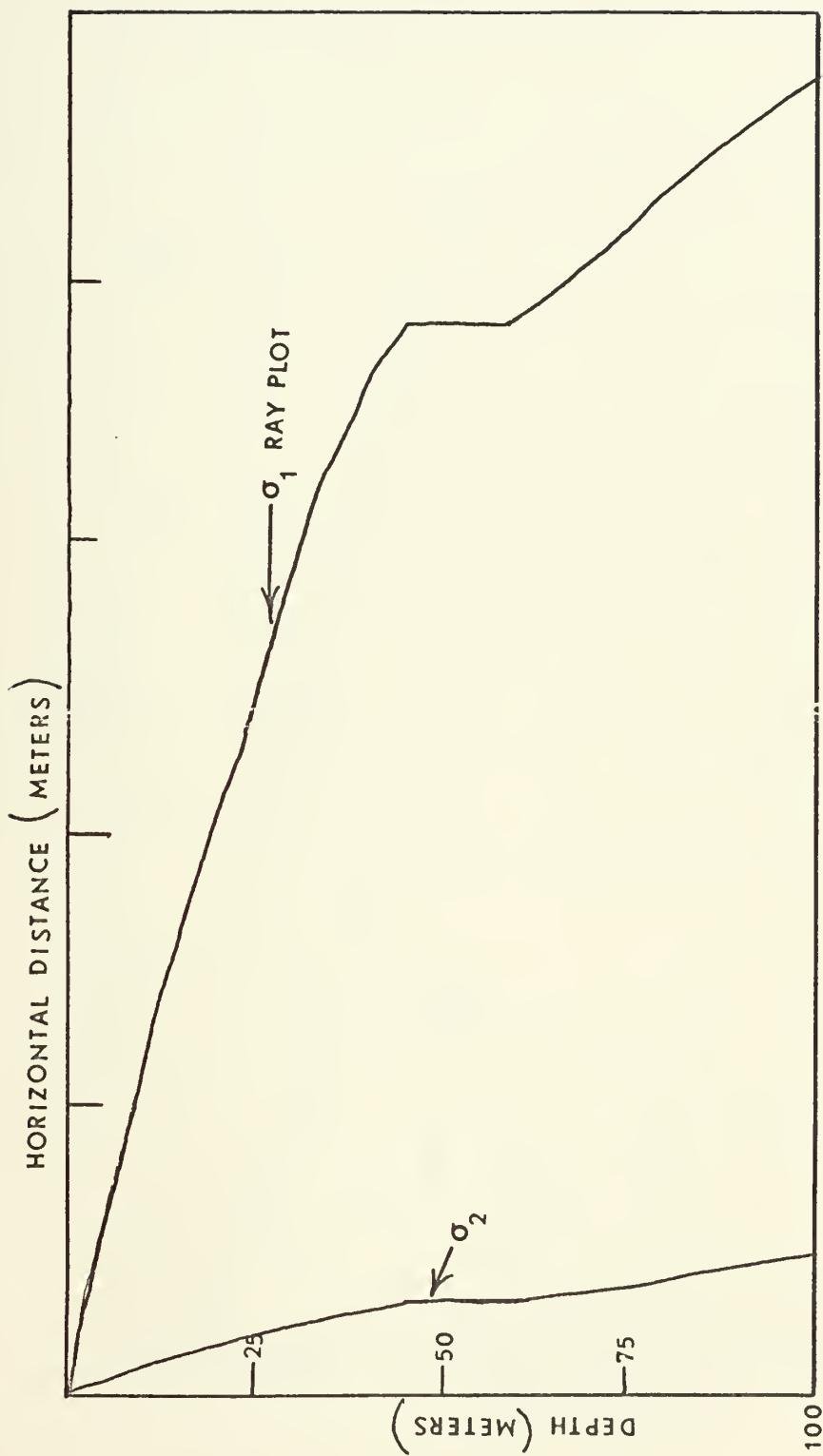


FIGURE 11. Ray plots for first two selected frequencies at the shallow station.



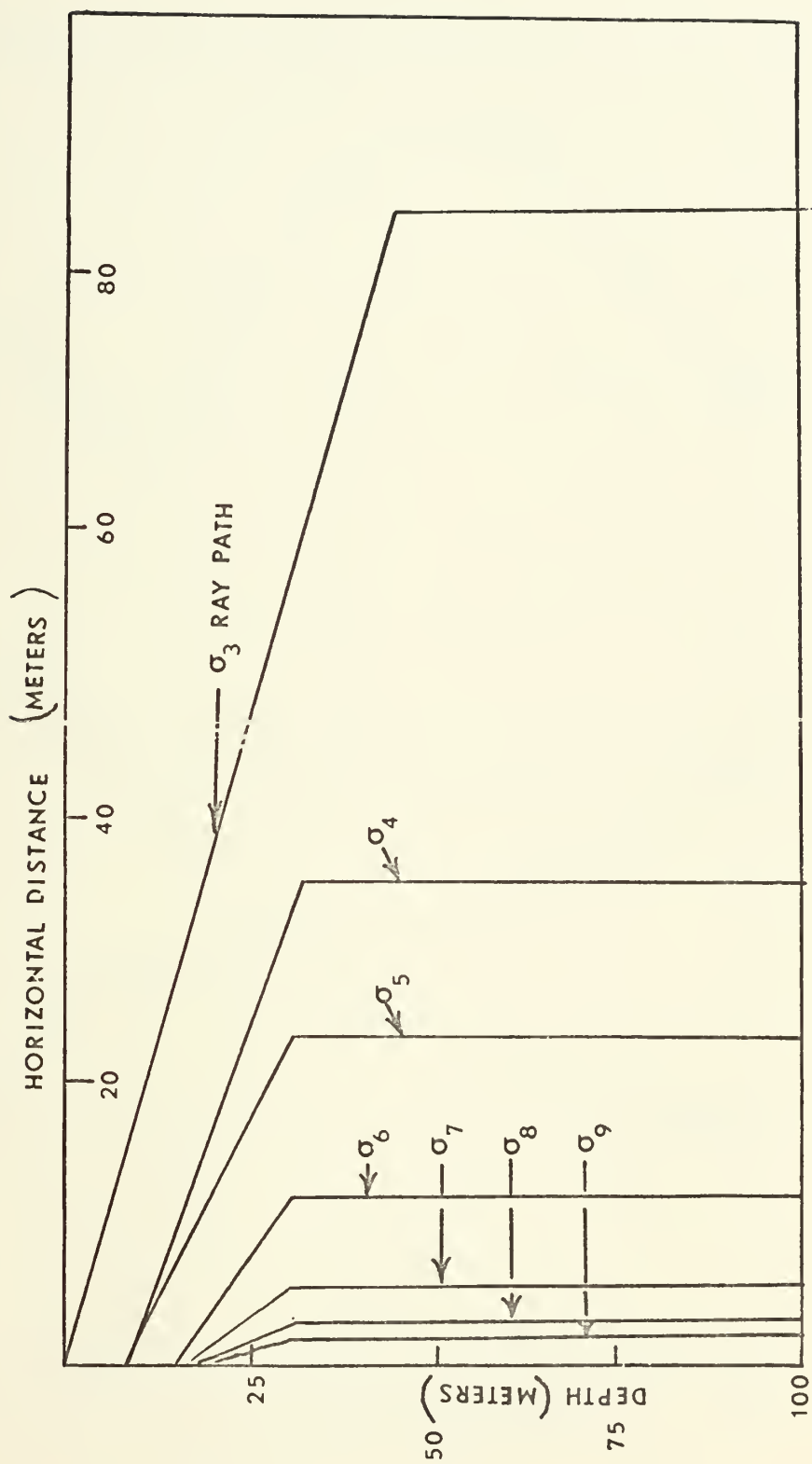


FIGURE 12. Ray plots for third through ninth frequencies at the shallow station



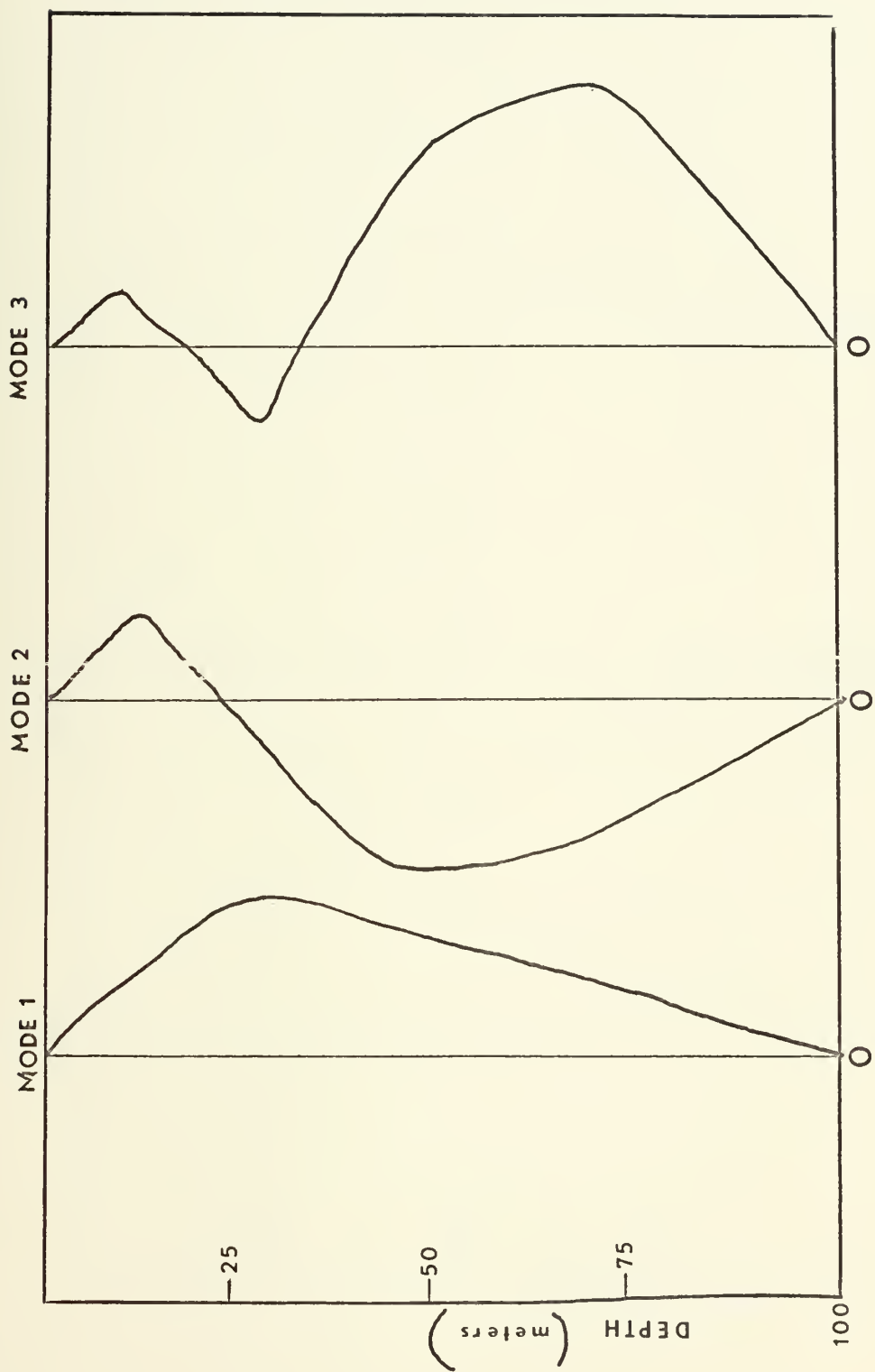


FIGURE 13. Modal structure for first selected frequency at shallow station





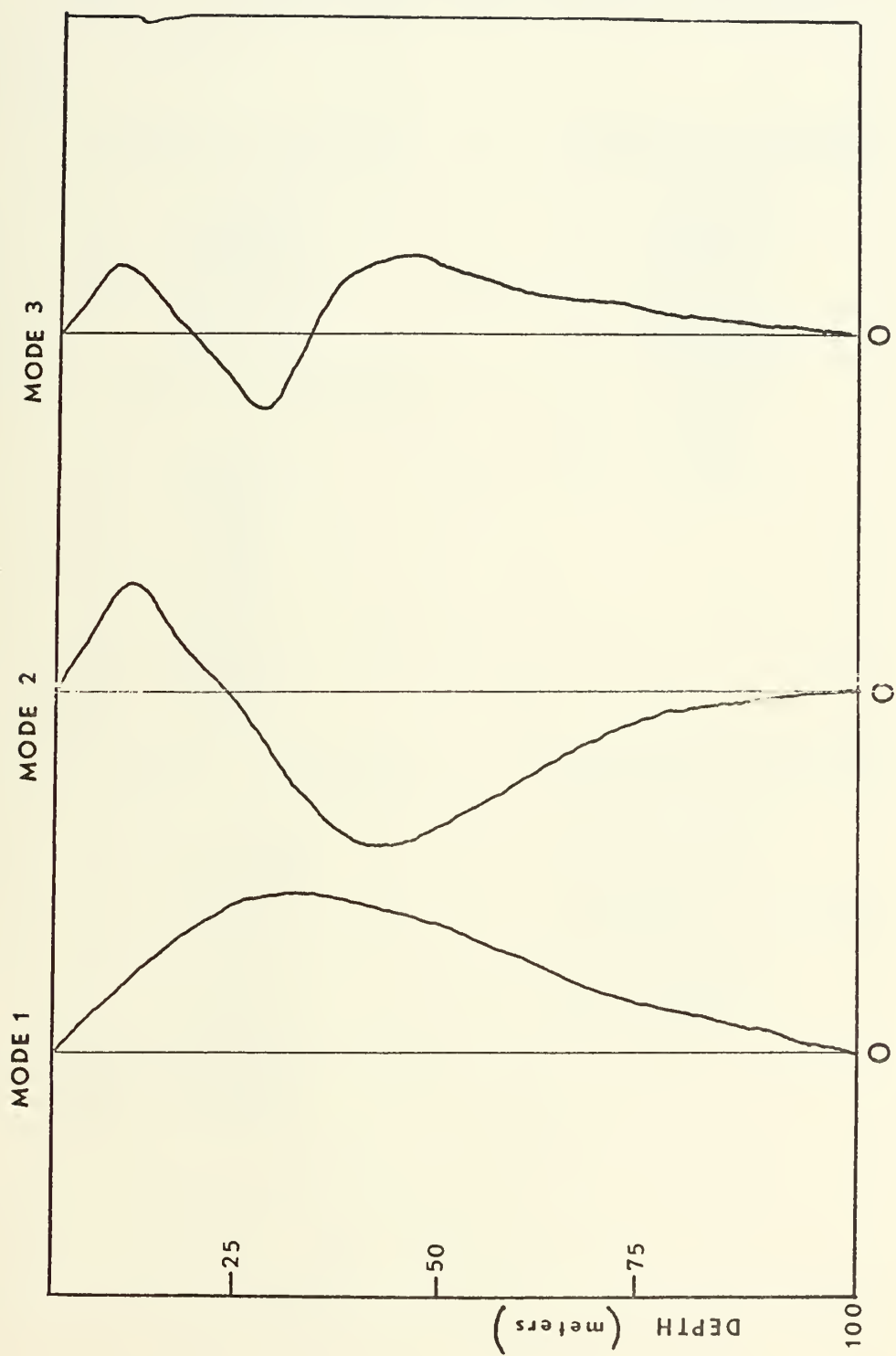


FIGURE 14. Modal structures for third selected frequency at shallow station



Table V. Normal modes for selected frequencies at the shallow station.

<u>0.01656 cycles/min.</u>	<u>0.15818 cycles/min.</u>
1. 0.00087701	1. 0.0086086
2. 0.0025324	2. 0.025461
3. 0.0035674	3. 0.041537
4. 0.0050806	4. 0.051653
5. 0.0055217	5. 0.069448
	6. 0.074546
	7. 0.092209
	8. 0.10860
	9. 0.12385
	10. 0.13605
<u>0.31554 cycles/min.</u>	
1. 0.018642	
2. 0.056013	
3. 0.10871	
4. 0.14614	
5. 0.17507	
6. 0.20301	
7. 0.23839	
8. 0.28283	
9. 0.33293	
10. 0.37399	
<u>0.47289 cycles/min.</u>	<u>0.63024 cycles/min.</u>
1. 0.032306	1. 0.053539
2. 0.094660	2. 0.14805
3. 0.19395	
4. 0.26040	
5. 0.33316	
6. 0.40811	
7. 0.48565	
8. 0.55884	
9. 0.63999	
10. 0.72820	
	<u>0.78760 cycles/min.</u>
	1. 0.092463
	2. 0.23132



## VI. CONCLUSIONS

The numerical program developed in this thesis has derived a technique that links the theoretical application of internal waves to real data. Real solutions are determined for actual density profiles. The program can yield a useful description of the internal wave regime within a given area. From representative samples of stations investigated, four points are apparent:

- (1), that with greater depth the effect of the boundary conditions weakens;
- (2), that for low frequencies that exceed the Vaisala frequency over only a small percentage of the water column, the ray path approaches the horizontal, while for higher frequencies the ray path approaches the vertical;
- (3), that the plot of the lowest three modes demonstrates the manner in which, with increasing frequency, the effect of the boundary conditions weakens as the oscillatory regions give way to exponential "decay" regions;
- (4), that for the stations investigated by this program, only those frequencies within the lower quarter of the inertio-gravity frequency band could be solved for normal modes with any degree of success.



## 46

UUUUUUUUUUUUUUUUUUUU    UUU    UUU    UU    UUUUUU                      UUUUU    U





```

104 WRITE(6,104) (Z(I),RHOSTA(I), I=1,M)
    FORMAT(48X,F7.1,19X,F7.5,/)
    CALL INTERP
    CALL RAY
    CALL RUNK
    C THE PROGRAM CONTINUES TO COMPUTE THE INTERNAL WAVE CHARACTERISTICS
    C UNTIL ALL STATION DATA HAVE BEEN READ.
    IDATA=IDATA-1
    IF (IDATA.GT.0) GO TO 20
    50 STOP
    END

```







[illegible]



```

DC 199 M=1,400
IF (VAISAL(M).LT.C0) VAISAL(M) = 0.
199 VAIS(M)=SQRT(VAISAL(M))
DO 11 J = 1,100
11 LINE(J) = DOT
WRITE(6,16) LINE
16 FORMAT(1,'',DEPTH(M) VAISALA FREQ. DENSITY',2X,10CAL1)
DO 21 N=2,100
11 LINE(N) = BLANK
DO 51 I=1,400,5
LINE(1) = DOT
FACTOR = (VAIS(I)/VASQRT)*100.
K = IFIX(FACTOR)
IF (K.LT.1) K=1
IF (K.GT.100) K=100
LINE(K)=STAR
STEP = ((RHO(I)-RHO(1))/(RHO(400)-RHO(1)))*100.
J = IFIX(STEP)
IF (J.LT.1) J=1
IF (J.GT.100) J=100
LINE(J) = AMP
WRITE(6,31) DEPTH(I),VAIS(I),RHO(I),LINE
31 FORMAT(2X,F6.1,1X,E13.4,3X,F7.5,1X,10CAL1)
LINE(K) = BLANK
LINE(J) = BLANK
51 CONTINUE
DO 15 I=1,100
SIGMA = FREQ(I)
SG = SIGMA**2
DO 65 J=2,100
65 LINE(J)=BLANK
SUM=0.
N=0
DELZ=ZMAX/400
DO 40 M=1,400
40 IF (SG.GT.VAISAL(M)) GO TO 20
10 RATIO(M) = (VAISAL(M)-SG)/(SG-(OMEGA/60.))**2)
GO TO 30
20 RATIO(M)=0.
N=N+1
30 ENTRY=SQRT(RATIO(M))*DELZ
SUM=SUM+ENTRY
40 S(M) = SUM
RN=N
PRCNT=RN/4.
WRITE(6,70) SUM
70 FORMAT(1,'',1X,DEPTH(M) EFFECT HOR. DIST.(M)',84X,F7.1,' METERS'
*)

```





```

DO 90 K=1,400,5
KK=1+K/5
S1(KK)=S(K)
IF (SUM.EQ.C.) GO TO 200
S(K)=(S(K)/SUM)*100.
GO TO 201
200 S(K)=0.
201 J=FIX(S(K))
IF (J.LT.1) J=1
IF (J.GT.100) J=100
LINE(1)=DOT
LINE(25)=DOT
LINE(50)=DOT
LINE(75)=DOT
LINE(100)=DOT
LINE(J)=STAR
IF (SG.GI.VAISAL(K)) GO TO 25
IF (SG.LE.VAISAL(K)) GO TO 35
35 WRITE(6,100) DEPTH(K),O,S1(KK),LINE
GO TO 45
25 WRITE (6,100) DEPTH(K),E,S1(KK),LINE
100 FORMAT(1X,F7.2,5X,A4,2X,F7.1,3X,100A1)
45 LINE(J)=BLANK
90 CONTINUE
SIG=SIGMA*60.
WRITE (6,50) SIG,PRCENT
50 FORMAT(' ',F4.1,'% OF THE TIME.')
15 CONTINUE
RETURN
END

```

IS GREATER THAN THE VAISALA FREQUENC







```

CAY=SIGMA/SQRT(G*ZMAX)
OMEGA = CMEGA/60.
BIG = 10.**20
EPS = 0.
NN = 1
JJ = 1
L=1
MM = 1
20 LL=1
590 Z1=0.
W1=0.
F1=-.0001
S1=0.
H=-ZMAX/20.
FEL = CAY**2/(SG-OMEGA**2)
DH=H/2.
W(1)=0.
DO 300 I=1,399,2
Z2=Z1+DH
W2=W1+F1*DH
F2=F1+S1*DH
CON=PHI(I)
S2=-CON*F2+FEL*(G*CON+SG)*W2
W3=W1+F2*DH
F3=F1+S2*DH
S3=-CON*F3+FEL*(G*CON+SG)*W3
W4=W1+F3*H
F4=F1+S3*H
CON=PHI(I+1)
S4=-CON*F4+FEL*(G*CON+SG)*W4
DY=H*(F1+2.*F2+2.*F3+F4)/6.
DF=H*(S1+2.*S2+2.*S3+S4)/6.
Z1=Z1+H
W1=W1+DY
F1=F1+DF
S1=-CON*F1+FEL*(G*CON+SG)*W1
J=(I+3)/2
IF (ABS(W1).GT.BIG) GO TO 309
IF (ABS(W1).GT.EPS) EPS = ABS(W1)
300 W(J)=W1
EPS = .005*EPS
ENDVAL=W(201)
KK=1
DO 301 M=1,199
301 IF (W(M)*W(M+1).LT.0.) KK=KK+1
315 IF (ABS(ENDVAL).LT.EPS) GO TO 350
306 IF (LL.EQ.1) GO TO 330
IF (ABS(W(201)).GT.ABS(W(200))) GO TO 308

```



```

307 GO TO 316
308 IF (KK.GT.1) GO TO 316
    CAY = CAY*.5
    GO TO 20
316 IF (STORE1.EQ.ENDVAL) GO TO 360
320 CAY=CAY-ENDVAL*(CAY2-CAY1)/(ENDVAL-STORE1)
    CAY1=CAY2
    CAY2=CAY
322 STORE1 = ENDVAL
    LL=LL+1
    IF (LL.EQ.21) GO TO 340
325 GO TO 590
330 STORE1=ENDVAL
    CAY1=CAY
    CAY2 = CAY*(1. + 0.1/L)
    CAY2 = CAY
    LL=LL+1
    GO TO 590
340 WRITE (6,345)
345 FORMAT(10X,' THE PROGRAM FAILS TO CONVERGE IN 20 ITERATIONS AND IS
    * PROCEEDING ON TO THE NEXT FREQUENCY.',/)
    GO TO 10
360 WRITE (6,365) L,CAY
365 FORMAT(10X,' VALUE OF MODE ',I2,' IS ',E14.7,' . APPROXIMATE VALUE
    * . EIGENFUNCTION NOT DETERMINED.',/)
    GO TO 378
350 M=1
    A=1
    B = 1
    DO 1 N=1,201
        IF (ABS(W(N)).LE.EPS) GO TO 1
        B = W(N)/ABS(W(N))
        IF (ABS(A-B).LT.0.5) GO TO 1
        M=M+1
    A = -A
1 CONTINUE
    IF (MM.EQ.2) GO TO 370
    IF (M.EQ.1) GO TO 400
    CAY = CAY/M
    GO TO 20
400 CAY = ABS(CAY)
    WRITE (6,410) CAY
410 FORMAT (10X,' VALUE OF MODE 1 IS ',E14.7,' .',/,)
    DO 415 IM = 1,201,3
        IN = 1 + IM/3
        WONE(IN) = W(IM)
        GUESS(1) = CAY
        GUESS(2)=2.*CAY

```





```

110 MM=2
155 L=L+1 GUESS(L)
370 GO TO 20
370 IF (M.LT.L) GO TO 115
370 IF (M.GT.L) GO TO 130
375 CAY = ABS(CAY)
375 WRITE(6,375) M,CAY
375 FORMAT(10X,' VALUE CF MODE ',I2,' IS ',E14.7,' ','/')
376 IF (L.EQ.2) GO TO 376
376 IF (L.EQ.3) GO TO 377
376 GO TO 378
376 DO 374 IM = 1,201,3
374 IN = 1 + IM/3
374 WTWO(IN) = W(IM)
377 GO TO 378
377 DO 373 IM = 1,201,3
377 IN = 1 + IM/3
373 WTHREE(IN) = W(IM)
373 WRITE(6,379)
379 FORMAT(' ','IX,DEPTH(M)',8X,'MODE ONE',28X,'MODE TWO',39X,'MODE TH
*REE',/)
380 WMAX1 = WONE(1)
380 WMAX2 = WTWO(1)
380 WMAX3 = WTHREE(1)
380 WMIN2 = WMAX2
380 WMIN3 = WMAX3
380 DO 380 N1 = 1,67
380 IF (WONE(N1).GT.WMAX1) WMAX1 = WONE(N1)
380 IF (WTWO(N1).GT.WMAX2) WMAX2 = WTWO(N1)
380 IF (WTHREE(N1).GT.WMAX3) WMAX3 = WTHREE(N1)
380 IF (WTHREE(N1).LT.WMIN3) WMIN3 = WTHREE(N1)
380 CONTINUE
380 DIFF2 = WMAX2 - WMIN2
380 DIFF3 = WMAX3 - WMIN3
380 DO 391 NM = 1,24
380 GRAPH1(NM) = BLANK
380 DO 392 NL = 1,49
380 GRAPH2(NL) = BLANK
380 GRAPH3(NL) = BLANK
380 DO 390 N2 = 1,57
380 STEP1 = (WONE(N2)/WMAX1)*24.
380 L1 = FIX(STEP1)
380 IF (L1.LT.1) L1 = 1
380 GRAPH1(1) = DOT
380 GRAPH1(L1) = ONE
380 IF (WTWO(N2).GT.0.) WTWO(N2) = ABS(WMIN2) + WTWO(N2)

```



```

IF (WTWO(N2).LE.C.) WTWO(N2) = ABS(WMIN2) - ABS(WTWO(N2))
STEP2 = (WTWO(N2)/DIFF2)*49.
L2 = IFIX(STEP2)
IF (L2.LT.1) L2 = 1
IF (N2.EQ.1) K2 = L2
GRAPH2(K2) = DOT
GRAPH2(L2) = TWO
IF (WTHREE(N2).GT.0.) WTHREE(N2) = ABS(WMIN3) + WTHREE(N2)
IF (WTHREE(N2).LE.C.) WTHREE(N2) = ABS(WMIN3) - ABS(WTHREE(N2))
STEP3 = (WTHREE(N2)/DIFF3)*49.
L3 = IFIX(STEP3)
IF (L3.LT.1) L3 = 1
IF (N2.EQ.1) K3 = L3
GRAPH3(K3) = DOT
GRAPH3(L3) = THREE
N3 = 6*N2 - 2
WRITE (6,395) DEPTH(N3),GRAPH1,GRAPH2,GRAPH3
FORMAT(1X,F6.1,1X,24A1,1X,49A1,1X,49A1)
GRAPH1(L1) = BLANK
GRAPH2(L2) = BLANK
GRAPH3(L3) = BLANK
CONTINUE
395
WRITE(6,393)
393
FORMAT(1,2CX,'COMPUTATION OF REMAINING SEVEN MODES.')
```

```

378
GUESS(L+1) = CAY
GUESS(L+1) = 2.*CAY-GUESS(L-1)
IF (L.EQ.10) GO TO 10
GO TO 110
105
IF (L.FQ.2) GO TO 120
115
CAY = 3.*GUESS(L-1) - 2.*GUESS(L-2)
NN = NN + 1
IF (NN.GT.10) GO TO 100
GO TO 20
130
RL = L
RM = M
CAY = CAY*(RL/RM)
JJ = JJ + 1
IF (JJ.GT.10) GO TO 100
GO TO 20
120
CAY = 1.5*GUESS(L)
GO TO 20
100
WRITE(6,160)
160
FORMAT(10X,'PROGRAM UNABLE TO DETERMINE CORRECT MODE. WILL PROCEED
* D TO NEXT FREQUENCY.')
```

```

309
WRITE(6,310)
310
FORMAT(10X,'VALUE OF W IS TOO HIGH. FURTHER MODES WILL BE ABORTED
* . PROGRAM WILL PROCEED TO NEXT FREQUENCY.')
```



10 CONTINUE  
RETURN  
END



## LIST OF REFERENCES

- Fjeldstad, J.E., "Interne Wellen." Geophys. Publ., Vol. 10, No. 6, pp. 1-35 (1933).
- LaFond, E.C., "Internal Waves, Part I." The Sea (Ed. M.N. Hill), Volume I, pp. 731-751 (1962).
- Oceanographic Cruise Report of Cruise NPS 1201-71, DeSteiguer (T-AGOR 12), August 10-20, 1970.
- Wunsch, C., and Dahlen, J., "Preliminary Results of Internal Wave Measurements in the Main Thermocline at Bermuda." Journal of Geophysical Research, Vol. 75, No. 30, pp. 5899-5908 (1970).
- Zalkan, R.L., Observation of High-Frequency Internal Waves in the Pacific Ocean, Ph.D. Thesis, University of California, San Diego, (1968).





# INITIAL DISTRIBUTION LIST

	No. Copies
1. Defense Documentation Center Cameron Station Alexandria, Virginia 22314	2
2. Library, Code 0212 Naval Postgraduate School Monterey, California 93940	2
3. Department of Oceanography, Code 58 Naval Postgraduate School Monterey, California 93940	3
4. Asst. Professor J.A. Galt Department of Oceanography, Code 58 Naval Postgraduate School Monterey, California 93940	3
5. Assoc. Professor J.J. von Schwind Department of Oceanography, Code 58 Naval Postgraduate School Monterey, California 93940	1
6. Oceanographer of the Navy The Madison Building 732 N. Washington Street Alexandria, Virginia 22314	1
7. Naval Oceanographic Office Attention: Library Washington, D.C. 20390	1
8. Dr. Ned Ostenso Office of Naval Research Code 480D Arlington, Virginia 22217	1
9. LCdr. W.J. Lounsbery KWESTEVDET Key West, Florida 33040	2
10. Lt. Jose Saldanha Instituto Hidrografico Ministerio da Marinha Lisboa, Portugal	1



## DOCUMENT CONTROL DATA - R &amp; D

(Security classification of title, body of abstract and indexing annotation must be entered when the overall report is classified)

1. ORIGINATING ACTIVITY (Corporate author) Naval Postgraduate School Monterey, California 93940		2a. REPORT SECURITY CLASSIFICATION Unclassified	
		2b. GROUP	
3. REPORT TITLE Response of a Water Column to Internal Waves of Known Frequencies			
4. DESCRIPTIVE NOTES (Type of report and, inclusive dates) Master's Thesis; September 1971			
5. AUTHOR(S) (First name, middle initial, last name) William J. Lounsbery			
6. REPORT DATE September 1971		7a. TOTAL NO. OF PAGES 60	7b. NO. OF REFS 5
8a. CONTRACT OR GRANT NO.		9a. ORIGINATOR'S REPORT NUMBER(S)	
b. PROJECT NO.			
c.		9b. OTHER REPORT NO(S) (Any other numbers that may be assigned this report)	
d.			
10. DISTRIBUTION STATEMENT Approved for public release; distribution unlimited.			
11. SUPPLEMENTARY NOTES		12. SPONSORING MILITARY ACTIVITY Naval Postgraduate School Monterey, California 93940	
13. ABSTRACT A program is developed to ascertain the response of a frictionless water column to internal waves. Using density strata as input, the program selects ten frequencies at equal intervals within a spectrum of internal waves bounded above by the maximum Vaisala frequency and below by the inertial frequency. Ray paths within the column are plotted for these frequencies. The first ten normal modes for each frequency are computed. The first three modes are plotted.			



## KEY WORDS

## LINK A

## LINK B

## LINK C

ROLE

WT

ROLE

WT

ROLE

WT

Internal waves  
Ray paths  
normal modes  
computer programs  
numerical methods



Thesis  
L827  
c.2

131205

Lounsbery

Response of a water  
column to internal  
waves of known  
frequencies.

Thesis  
L827  
c.2

131205

Lounsbery

Response of a water  
column to internal  
waves of known  
frequencies.

thesL827

Response of a water column to internal w



3 2768 002 12674 0

DUDLEY KNOX LIBRARY